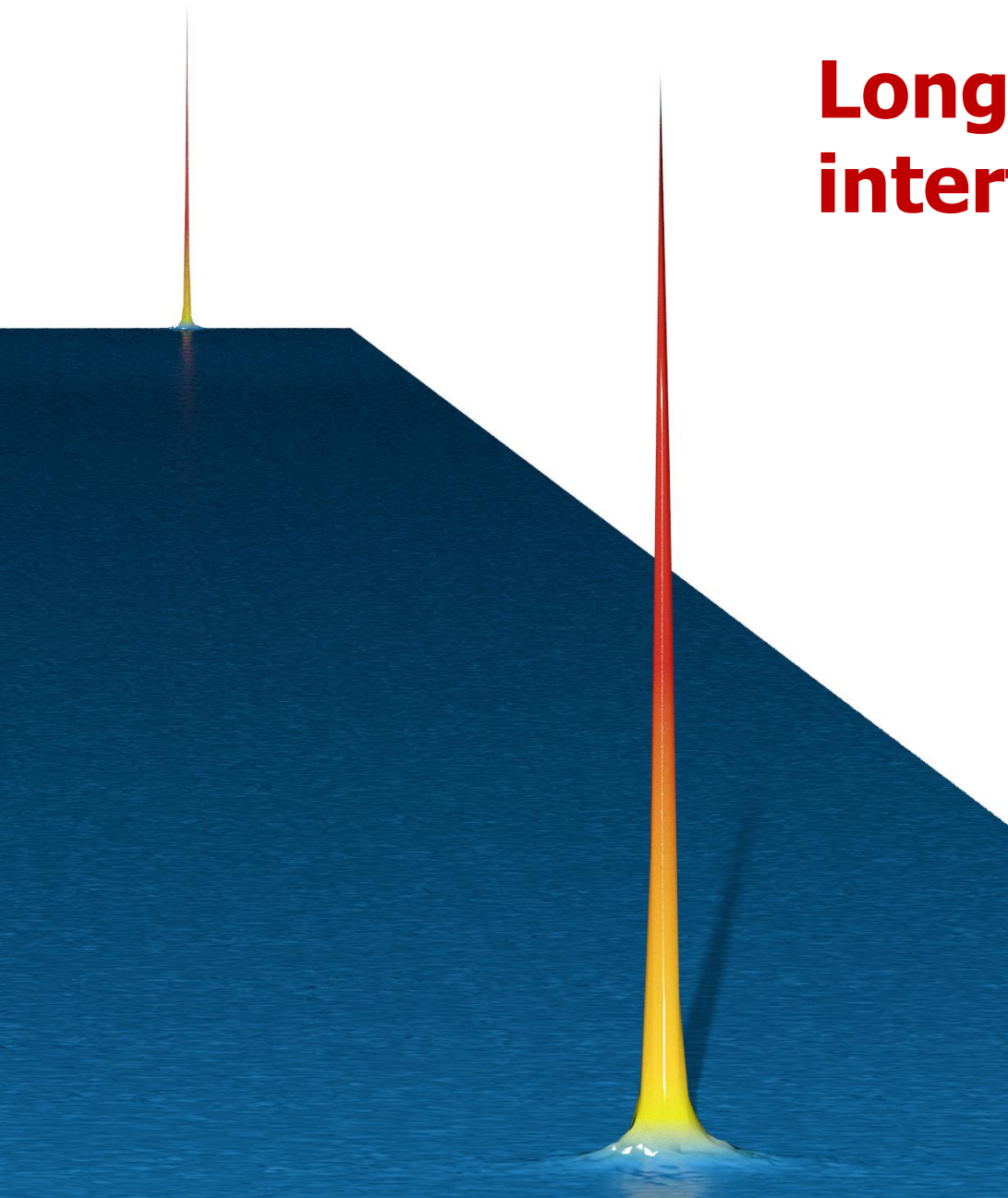


Long baseline atom interferometry

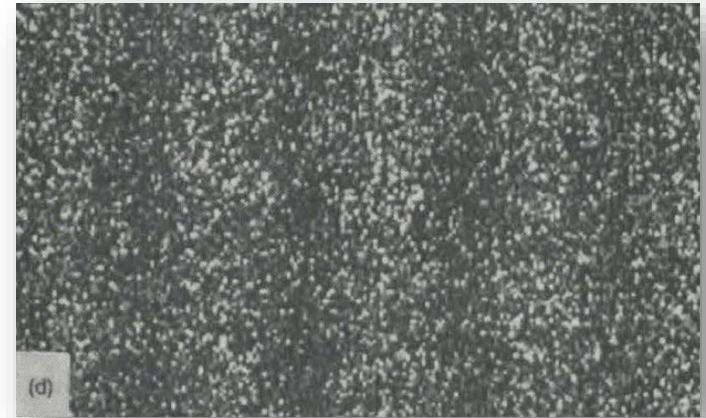
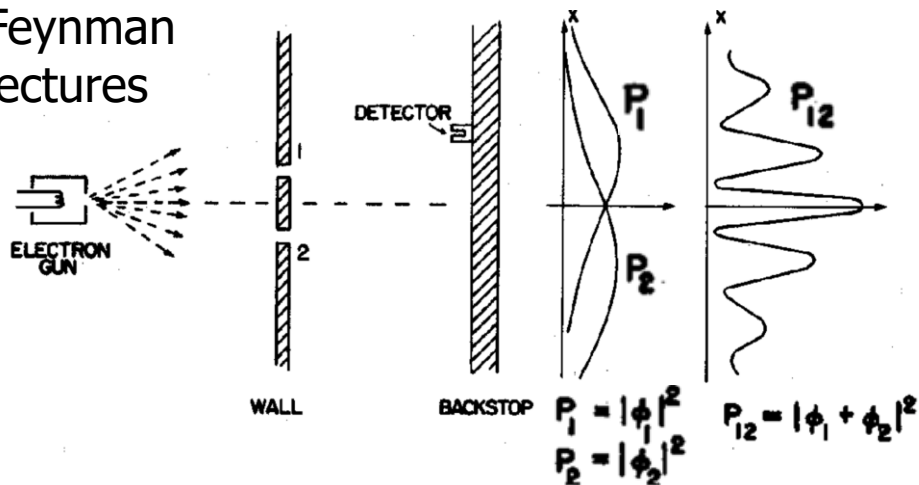


Mark Kasevich
Stanford University
kasevich@stanford.edu

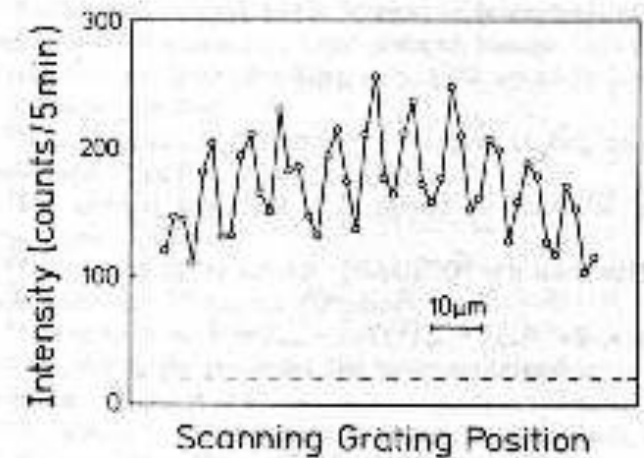
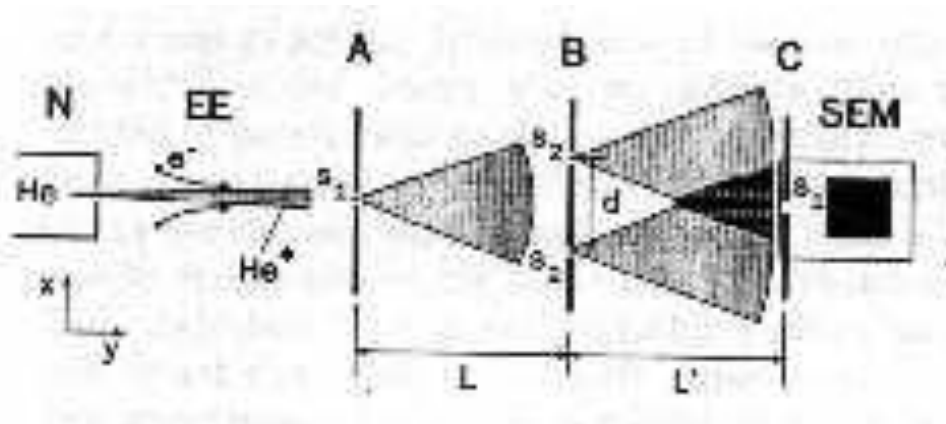


Young's double slit exp't with particles

Feynman lectures

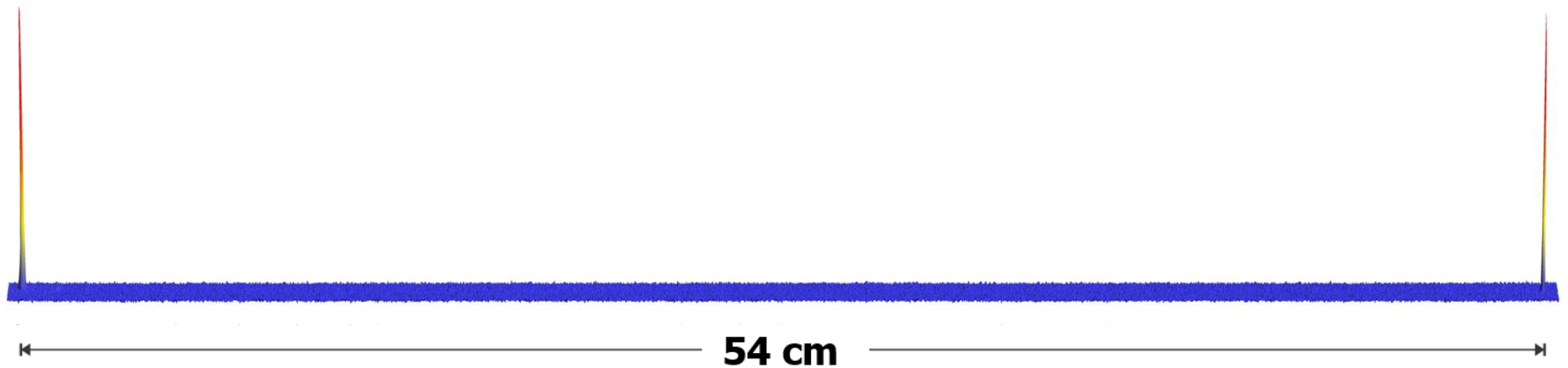


Tomomura, PRL, 1989



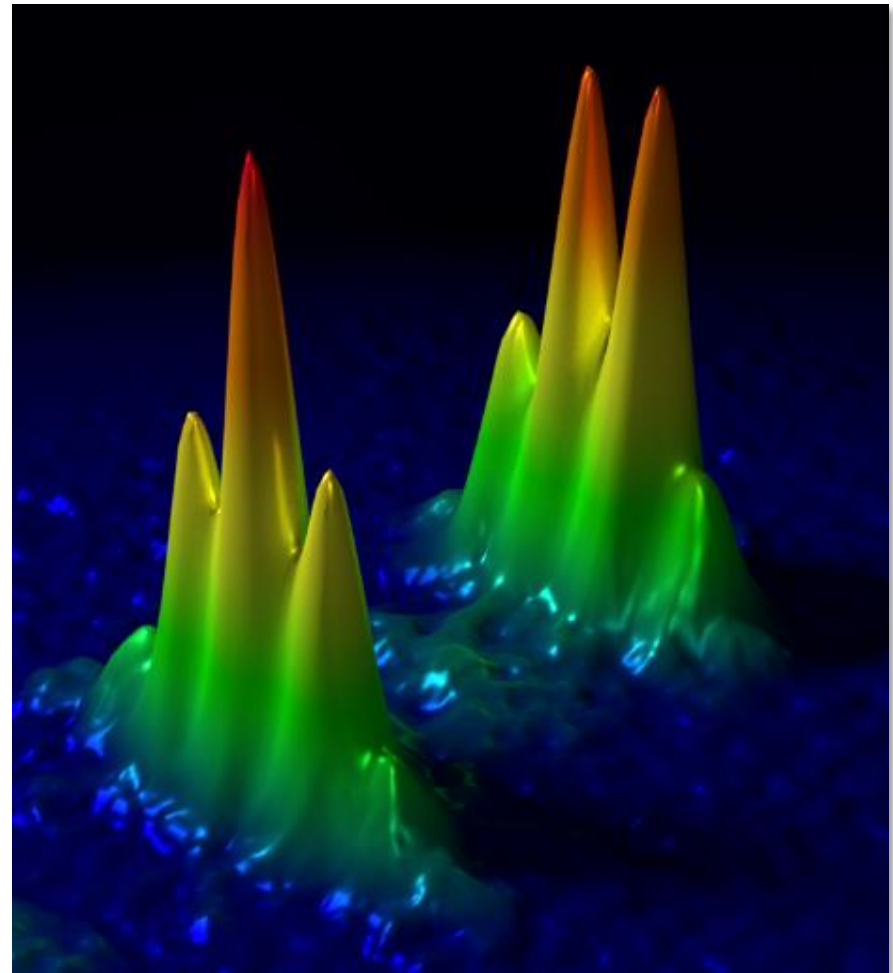
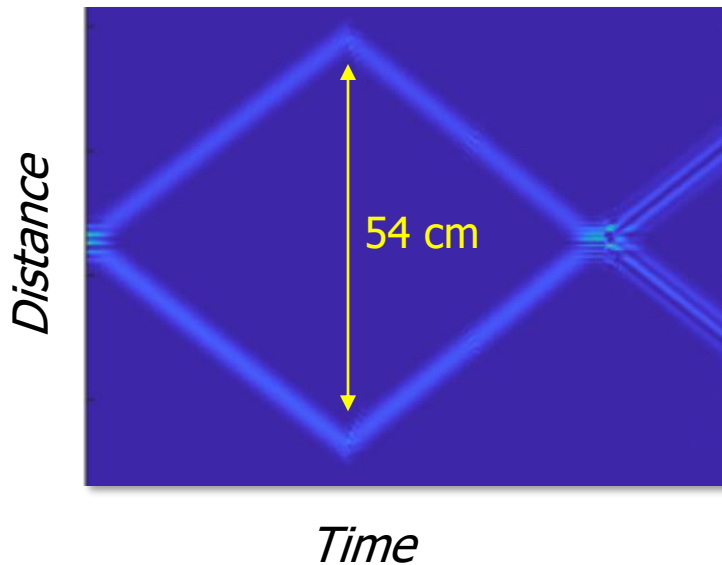
Mlynek, PRL, 1991

Atomic wavepacket superposition



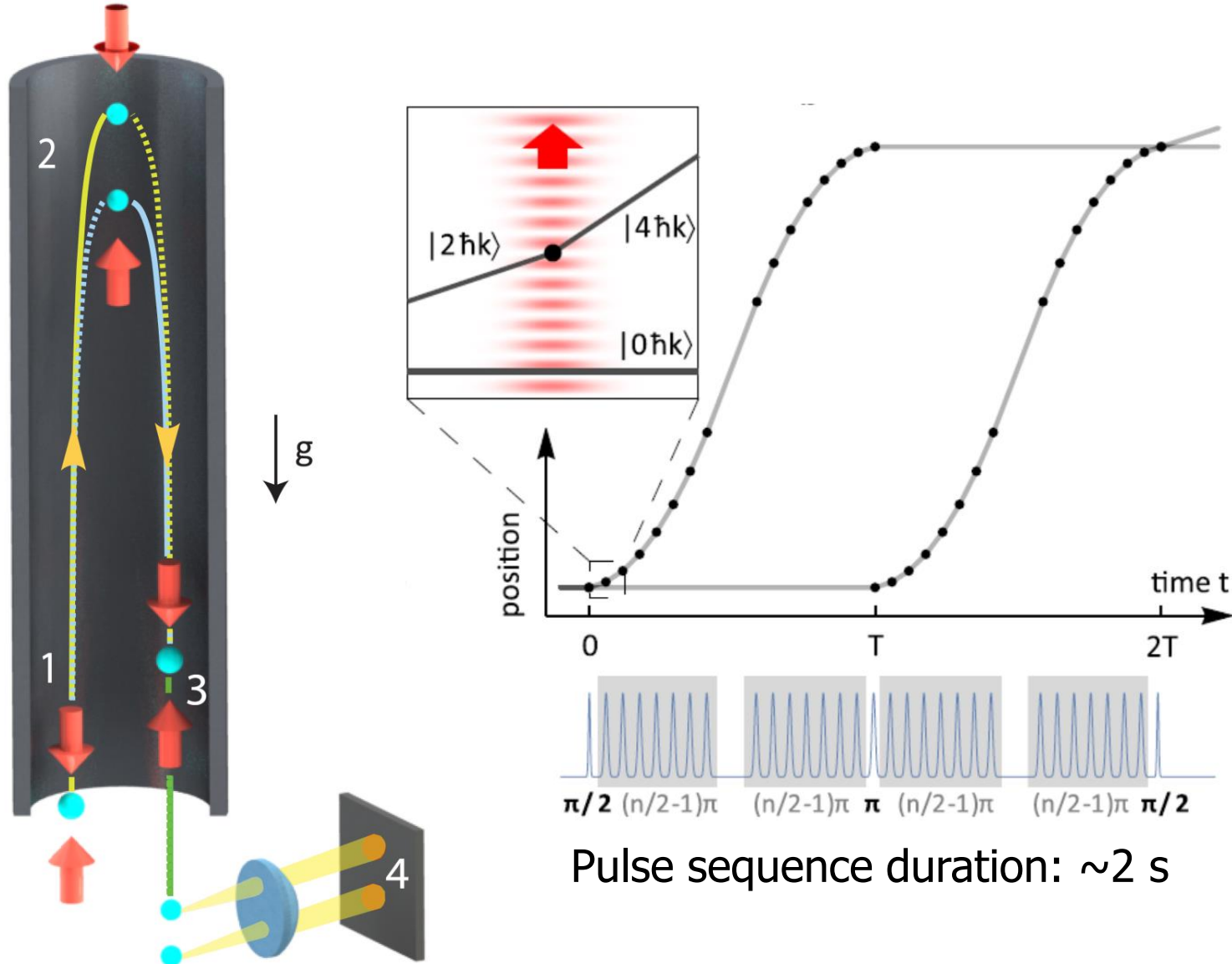
Atomic wavepacket interference

Interferometer atomic
center-of-mass wavefunction



Superposed atomic wavepackets interfere

Light pulse atom interferometry

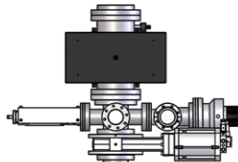


Pulse sequence duration: ~ 2 s

Apparatus

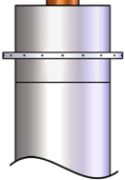


Atom Optics & Lattice Beam
Delivery Enclosure

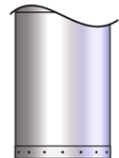


Upper Detection Region

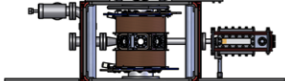
Interferometer Region
8.2 m



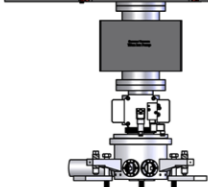
3 Layer Magnetic Shield
(<1 mG on axis)



Lower Detection Region



2D MOT Loading 3D



Rotation Compensation
System

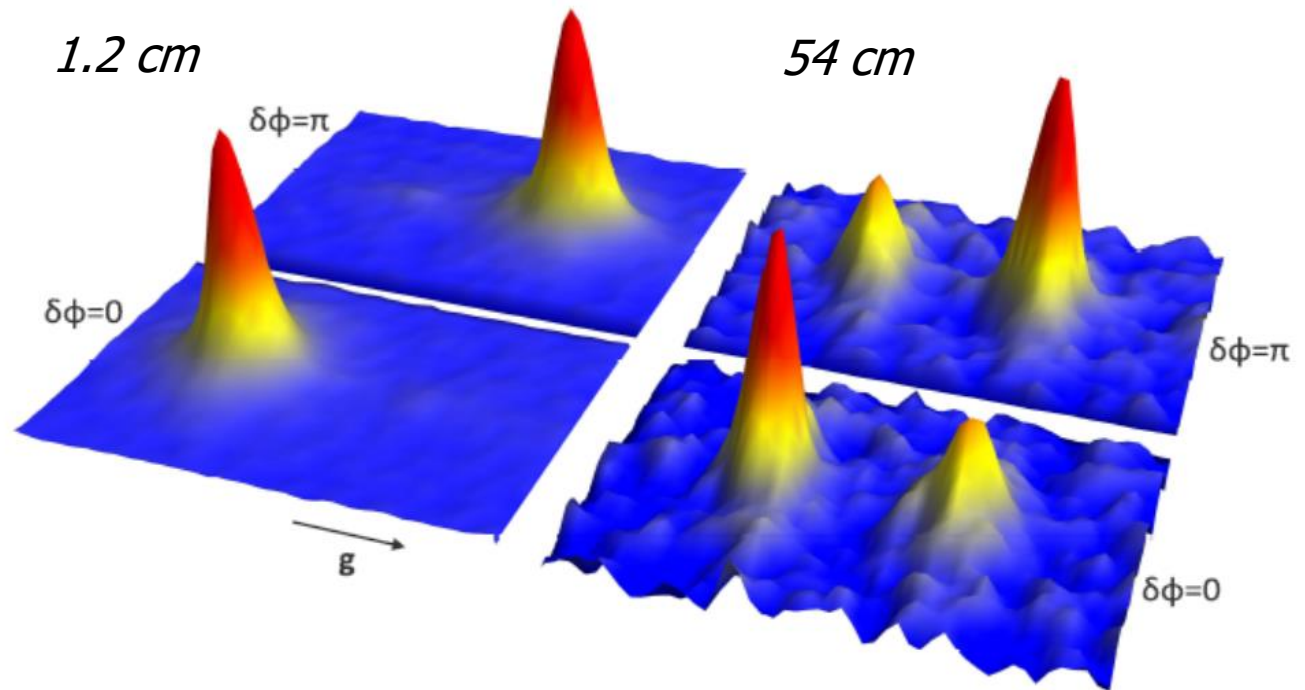
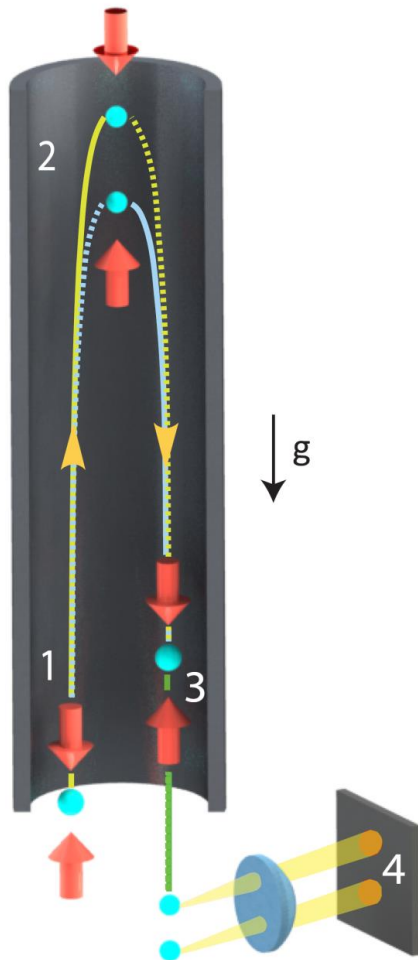
1 m



~ 100 pK
 $1e5$ atoms/shot



Interference at output ports



Interference causes population modulation between the output ports

Bounds for gravitational decoherence

IOP Publishing

Classical and Quantum Gravity

Class. Quantum Grav. 35 (2018) 145005 (18pp)

<https://doi.org/10.1088/1361-6382/aac72f>

Gravity is not a pairwise local classical channel

$$\tilde{\Gamma}_{\text{KTM}}^C = C \frac{GMm}{\hbar R^3} \Delta x^2$$

Natacha Altamirano^{1,2}, Paulina Corona-Ugalde^{2,3},
Robert B Mann^{1,2,3} and Magdalena Zych^{4,5}

Experiment	m (Kg)	M (Kg)	d (m)	Δx (m)	$1/\Gamma_{\text{DP}}$ (s)	$1/\Gamma_{\text{KTM}}^{\text{min}}$ (s)
10 m atomic fountain with ^{87}Rb [38]	1.4×10^{-25}	M_{\oplus}	R_{\oplus}	0.54	3×10^{10}	2×10^{-3}
Two atomic fountains with ^{87}Rb [33] (Operating as gravity-gradiometer)	1.4×10^{-25}	M_{\oplus}	R_{\oplus}	1.86×10^{-3}	3×10^{10}	2×10^1
		4×129	0.11, 0.18, 0.28, 0.31			
Large-molecule interferometry [43]	1.6×10^{-23}	M_{\oplus}	R_{\oplus}	2.7×10^{-7}	3×10^6	6×10^7
PcH ₂ diffraction on alga skeleton [44]	8.2×10^{-25}	M_{\oplus}	R_{\oplus}	2×10^{-7}	1×10^9	2×10^9

Large wavepacket separation AI constrains the KTM model



Phase shifts (non-relativistic)

Term	Phase Shift	
1	$k_{\text{eff}} g T^2$	Gravity
2	$2\mathbf{k}_{\text{eff}} \cdot (\boldsymbol{\Omega} \times \mathbf{v}) T^2$	Coriolis
3	$k_{\text{eff}} v_z \delta T$	Timing asymmetry
4	$\frac{\hbar k_{\text{eff}}^2}{2m} T_{zz} T^3$	Curvature, quantum (tidal)
5	$k_{\text{eff}} T_{zi} (x_i + v_i T) T^2$	Gravity gradient
6	$\frac{1}{2} k_{\text{eff}} \alpha (v_x^2 + v_y^2) T^2$	Wavefront

8e9 rad



T_{ij} , gravity gradient

v_i , velocity; x_i , initial position

g , acceleration due to gravity

T , interrogation time

k_{eff} , effective propagation vector



Equivalence Principle

Acceleration of co-falling ^{85}Rb and ^{87}Rb ensembles is measured using light-pulse atom interferometry

Statistical sensitivity

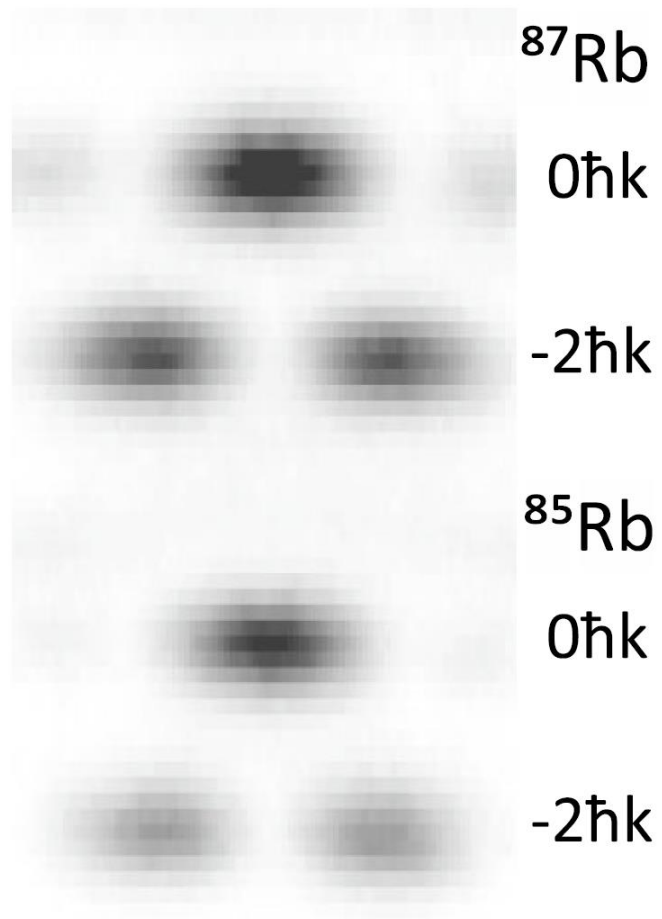
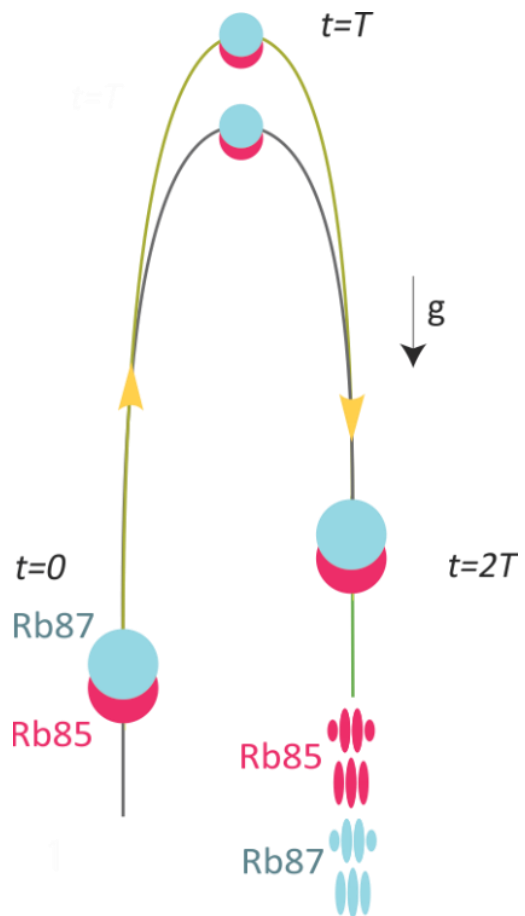
$\delta g \sim 10^{-15} \text{ g}$ with 1 month data collection.

Limited by atom number.

Systematic uncertainties

$\delta g/g \sim 10^{-14}$ limited by magnetic field inhomogeneities, gravity anomalies, and light-shifts.

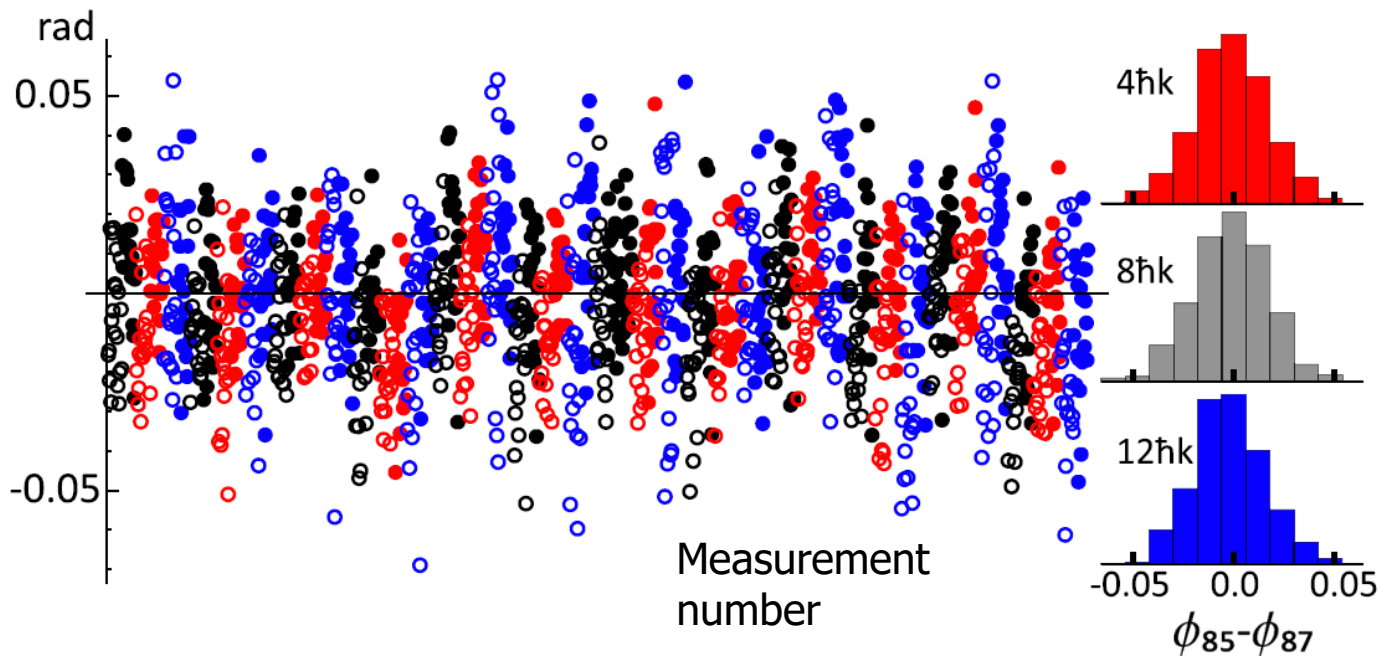




Data

The differential accelerations of ^{85}Rb and ^{87}Rb are inferred by comparing phase shifts for atom interferometers with differing wavepacket separation (recoil momenta).

This suppresses systematic phase shifts associated with the initial and final beam-splitting interactions.



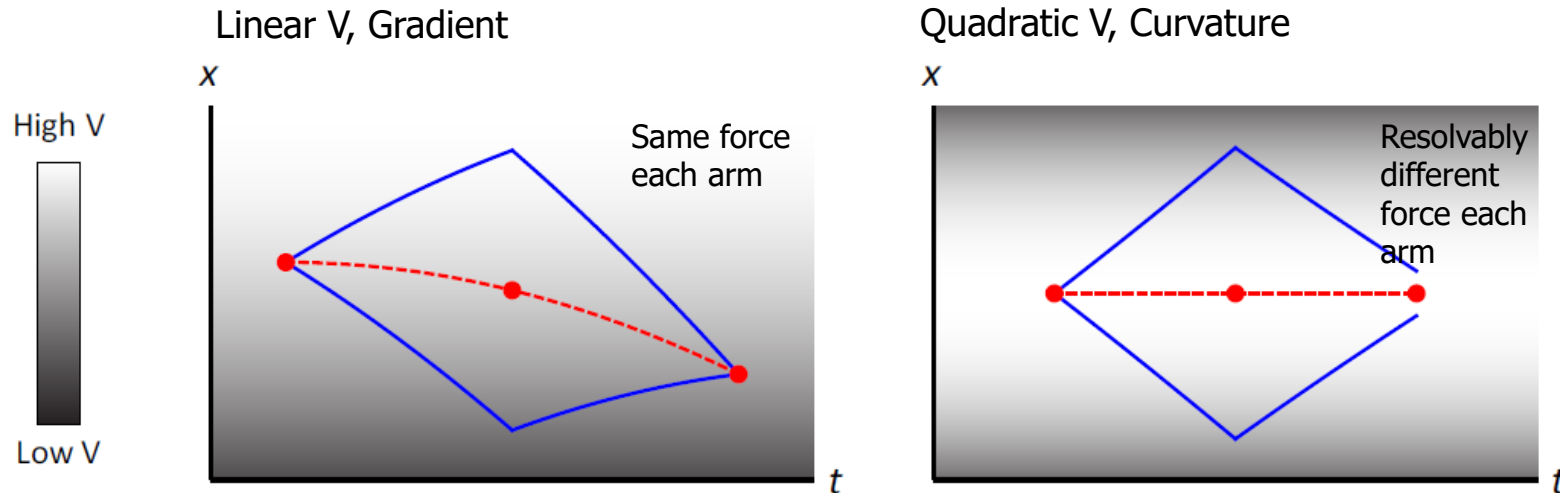
Equivalence Principle Test Results

$$\eta = [1.6 \pm 1.8(\text{stat}) \pm 3.4(\text{syst})] \times 10^{-12}$$

Parameter	Shift	Uncertainty
Total kinematic	1.5	2.0
Δz		1.0
Δv_z	1.5	0.7
Δx		0.04
Δv_x		0.04
Δy		0.2
Δv_y		0.2
Width		1.6
ac-Stark shift		2.7
Magnetic gradient	−5.9	0.5
Pulse timing		0.04
Blackbody radiation		0.01
Total systematic	−4.4	3.4
Statistical		1.8



Atom interferometer vs. classical measurements



In both cases, interferometer phase shift is well described by the classical trajectories associated with the interferometer arms:

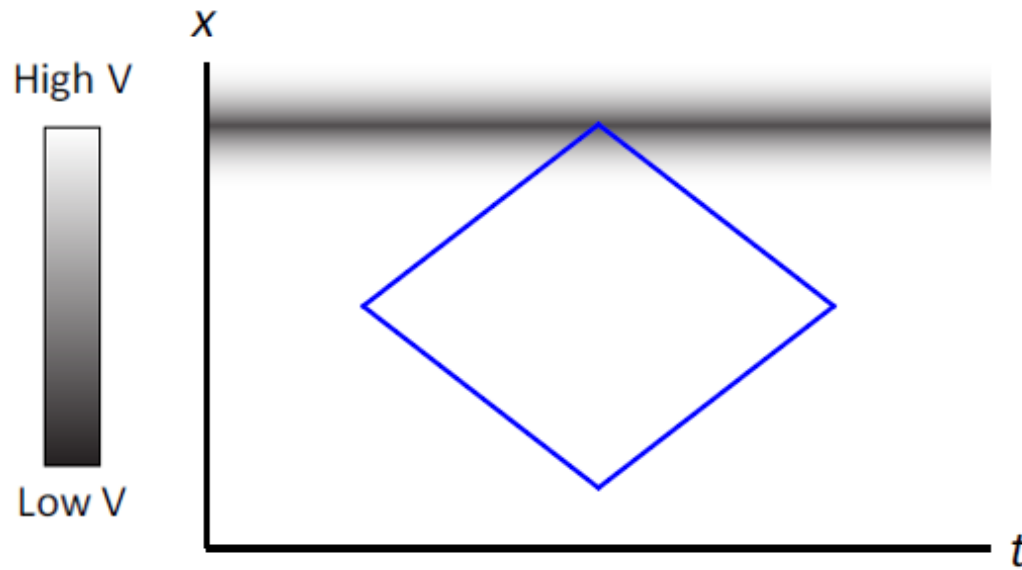
$$\phi_{\text{MP}} \equiv \sum_{i=1}^N [(k_{1,i} - k_{2,i}) \bar{x}_i - (\omega_{1,i} - \omega_{2,i}) t_i + (\phi_{1,i} - \phi_{2,i})].$$

(k_i and x_i are propagation vectors and wavepacket positions at the i^{th} pulse.)

These atom interferometric measurements are conceptually similar to classical measurements. Phase shift is given by the force acting on atomic wavepackets.



Mass dependent phase shifts



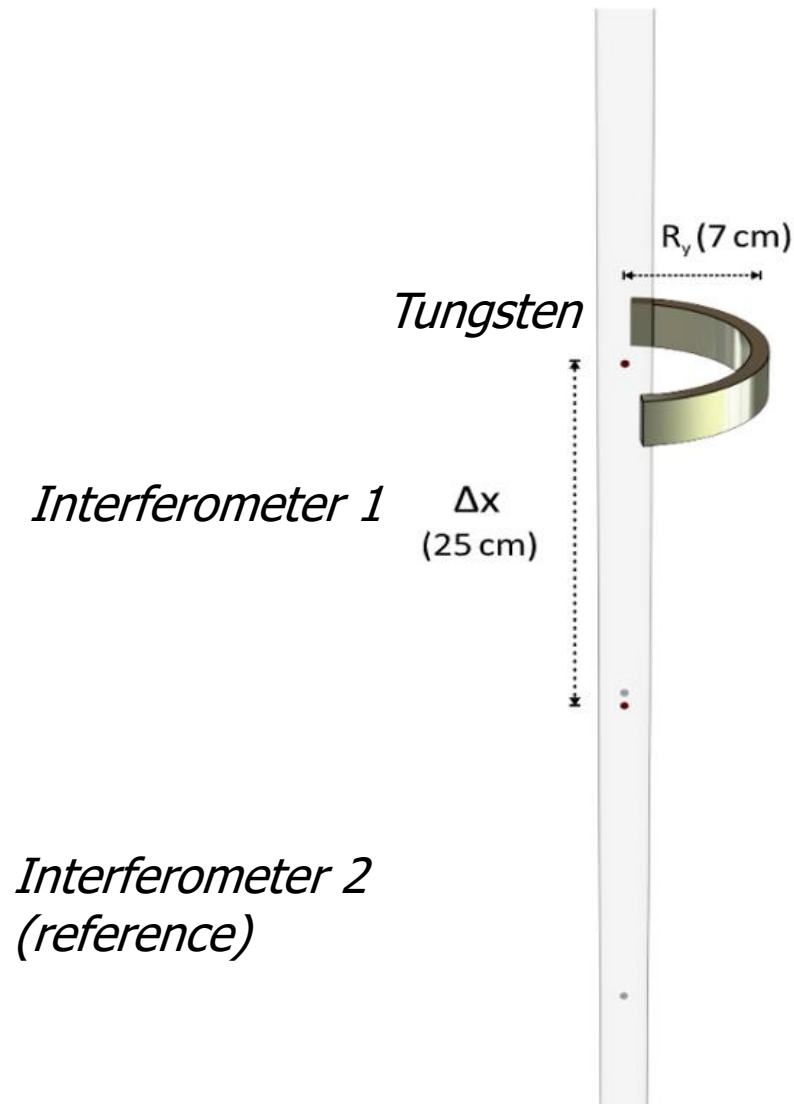
For higher order curvature, the phase shift is mass dependent.

Can be interpreted as a gravitational Aharonov-Bohm effect.

Possible systematic for future EP measurements based on atom interferometry.



Gravitational Aharonov-Bohm Experiment



Wavepacket separation greater than distance of nearest wavepacket to source mass

Overstreet, et al., Science, 2022

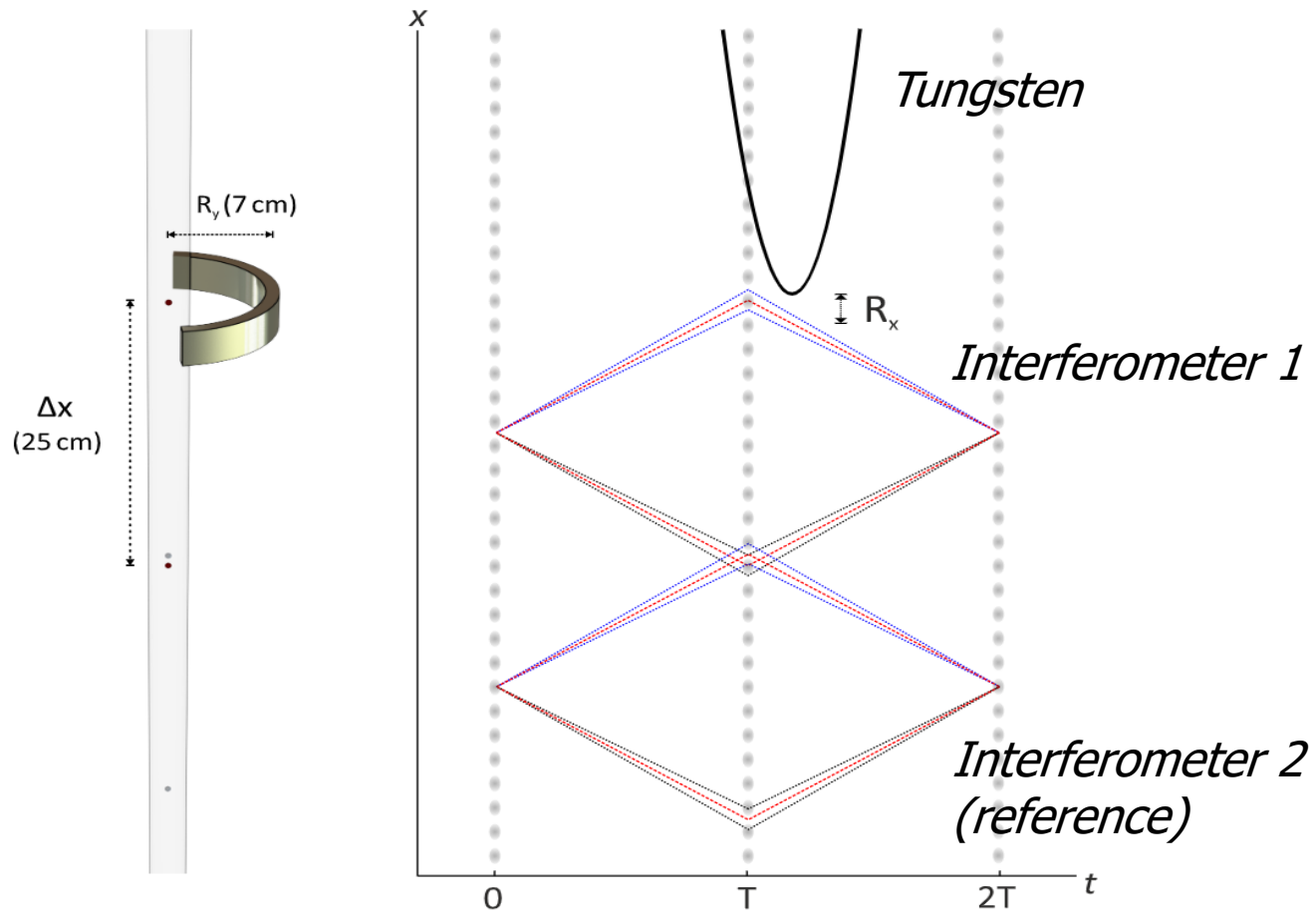
Prior proposals:

Audretsch and Lammerzhall, 1983

Hohensee, et al., 2012

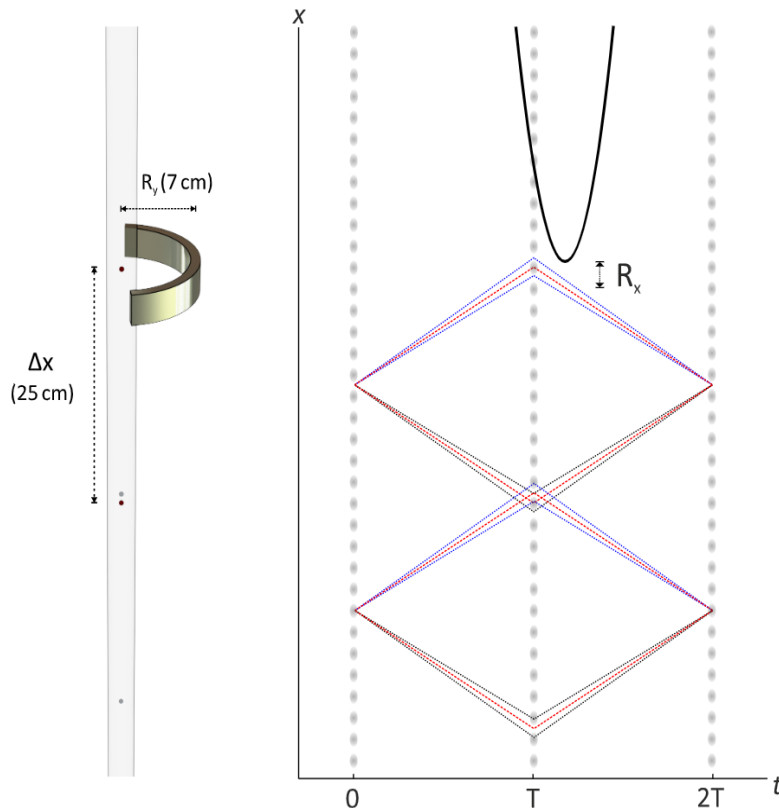


Interferometer trajectories in freely falling frame



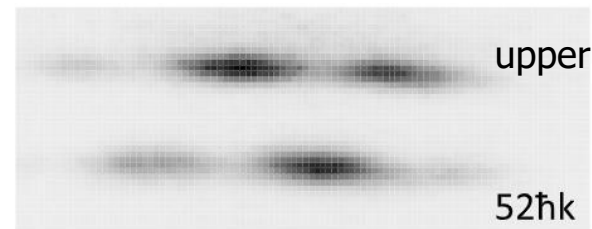
Phase shift due to gravitational action

Interferometer geometry

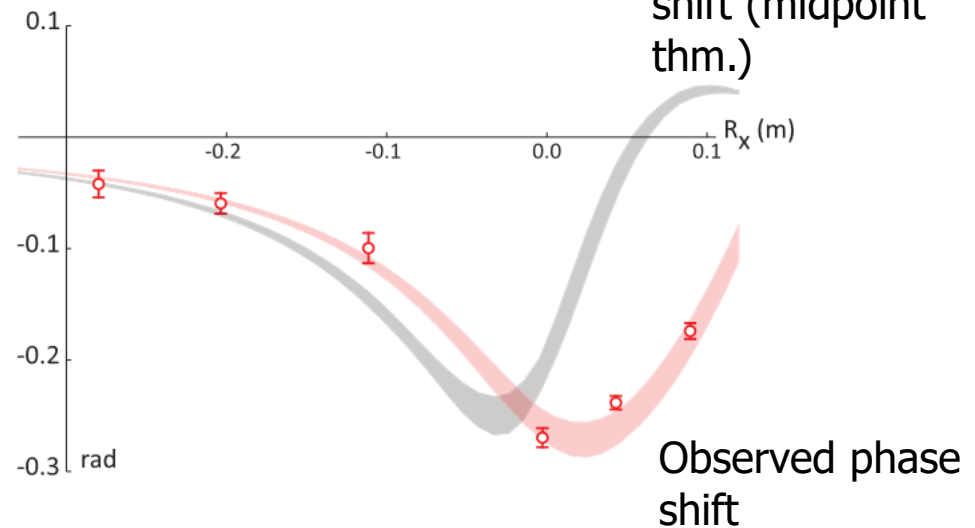


($\sim 7e-12$ g/shot resolution for each accelerometer)

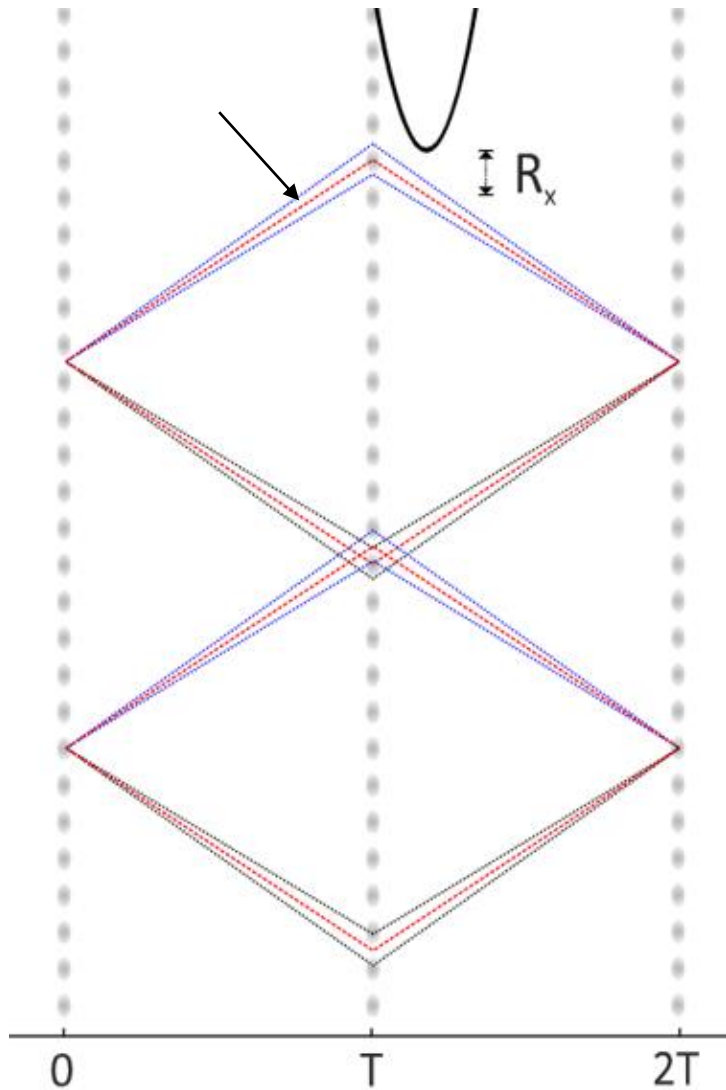
Raw data



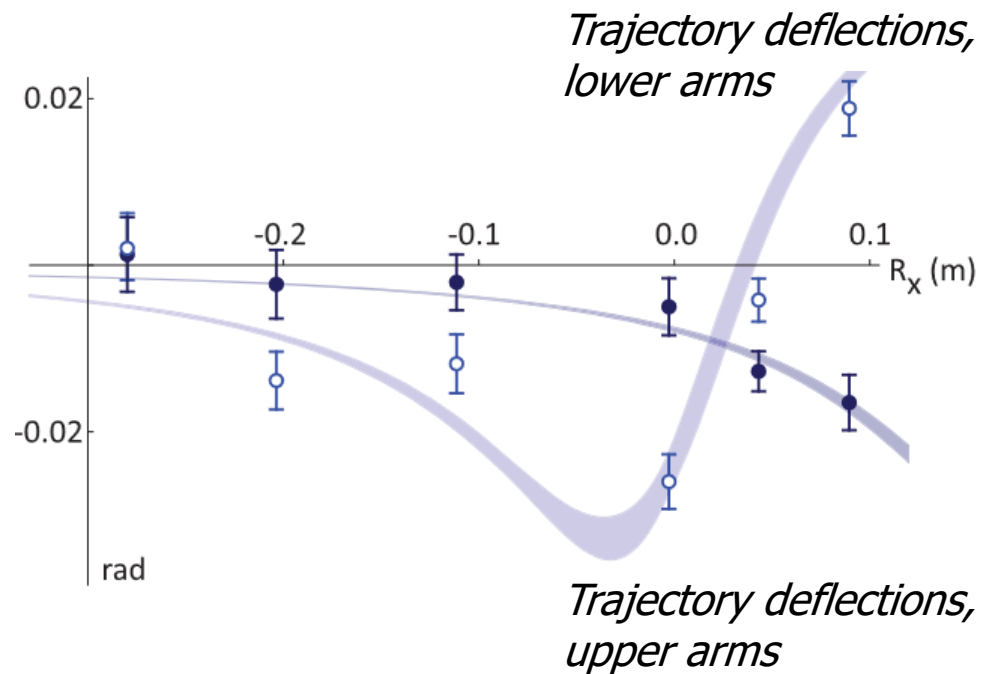
Phase shift



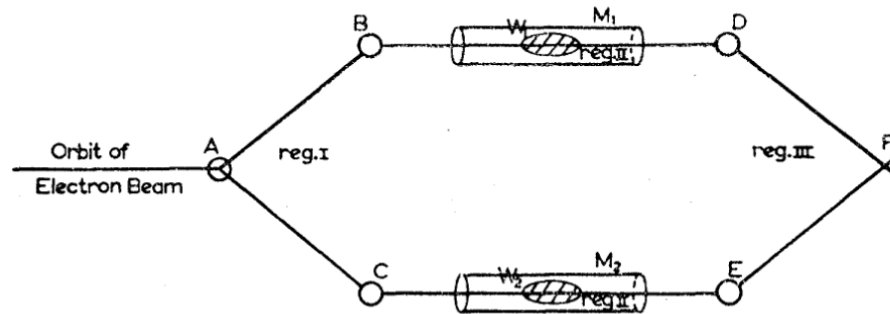
Deflection-induced phase shifts



Auxiliary (small wavepacket separation) interferometers allow independent characterization of deflection-induced phase shifts



Scalar Aharonov-Bohm Effect



Aharonov and
Bohm, Phys.
Rev. 1959

$$\psi = \psi_1^0 e^{-iS_1/\hbar} + \psi_2^0 e^{-iS_2/\hbar}$$

$$S_1 = e \int \varphi_1 dt, \quad S_2 = e \int \varphi_2 dt.$$

Negligible contribution to phase shift from forces on wavepackets (!)

One interpretation: physical original of the phase shift is the energy required to establish potential in the presence of the electron's electric field. Implies electron electric field is in superposition.

By analogy, observation of the gravitational Aharonov-Bohm shift implies the atom's gravitational field is in superposition.



Newtonian gravitational field energy

Field energy (weak field limit):

$$E_G = -\frac{1}{8\pi G} \int |\mathbf{g}|^2 dV$$

$$\mathbf{g} = \mathbf{g}_{\text{atom}} + \mathbf{g}_{\text{tungsten}}$$

Phase shift:

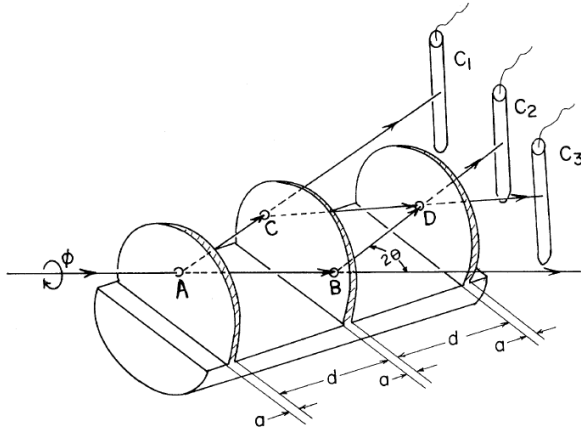
$$\phi = \frac{1}{\hbar} \int (E_1 - E_2) dt$$

E_1, E_2 are gravitational energies for each arm.

Phase shift is interpreted as resulting from energy stored in superposed gravitational fields.

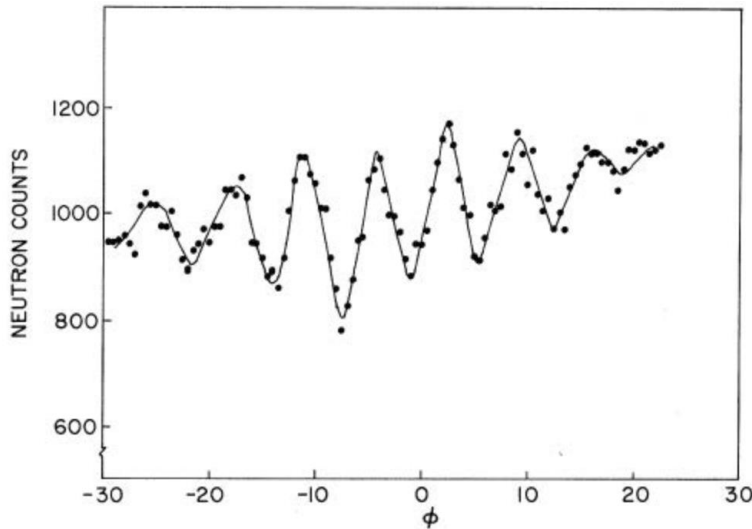


Collela, Overhauser and Werner (1975)



Uniform gravitational field implies gravitational action phase shift is zero -- uniform gravitational fields are not observable.

Physical origin of phase shift: relative (kinematic) displacement of Si crystal with respect to de Broglie waves due to non-gravitational forces.*



*textbook treatments use perturbation theory, which masks the physical origin of the phase shift.



(Very) long baseline sensors

Exploit sensitivity for fundamental physics by comparing outputs of distant atom interferometers

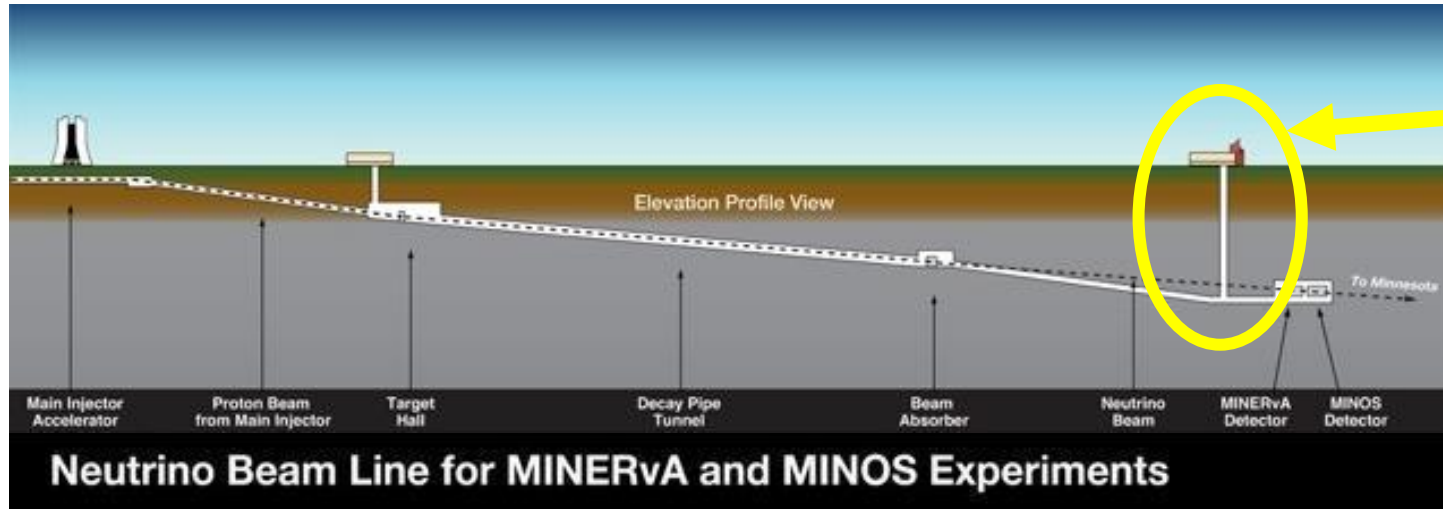
- gravitational wave detection
- ultra-light dark matter detection

Physics reach scales with separation of interferometers



- $L \sim 100 - 1000+$ m for envisioned ground-based detectors
- Precision atom interferometers at each end of the baseline
- Separation limited by Earth rotation and seismic noise

MAGIS-100: Detector prototype at Fermilab



MINOS
access shaft

Atom source

Atom source

Atom source

100m

- 100-meter baseline atom interferometry in existing shaft at Fermilab
- Intermediate step to full-scale (km) detector for gravitational waves
- Atom sources (Sr) at three positions to realize a gradiometer
- Probes for ultralight scalar dark matter beyond current limits (Hz range)
- Extreme quantum superposition states: >meter wavepacket separation



Northwestern
University

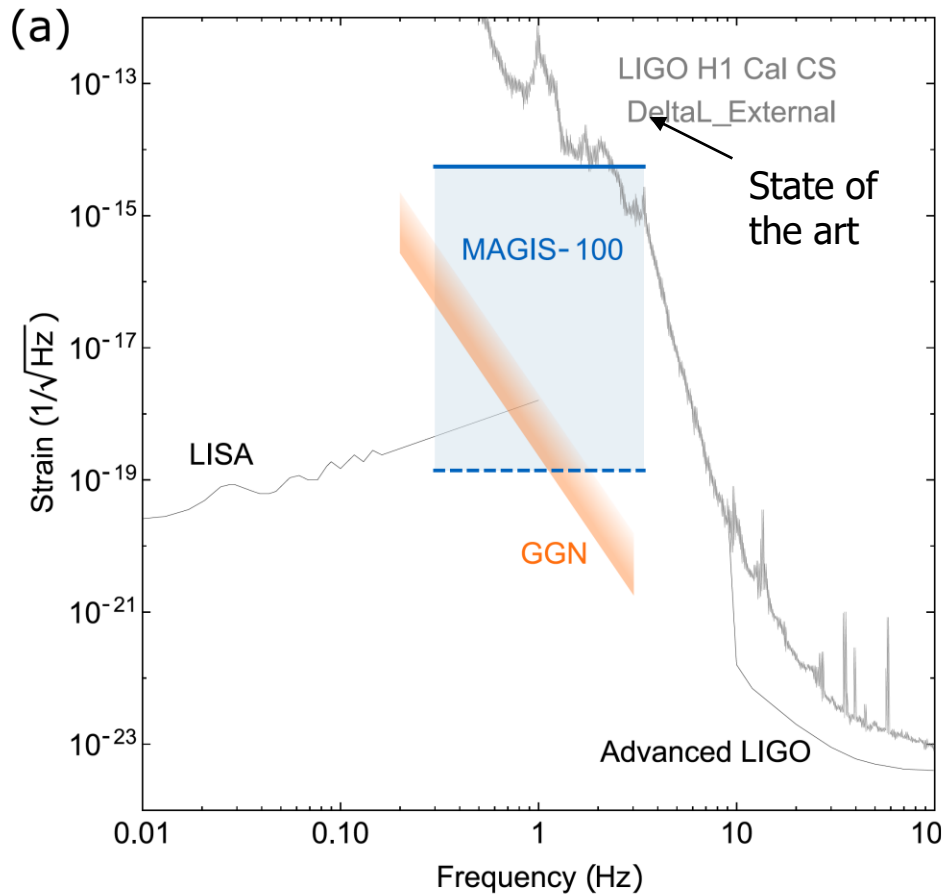


Fermilab

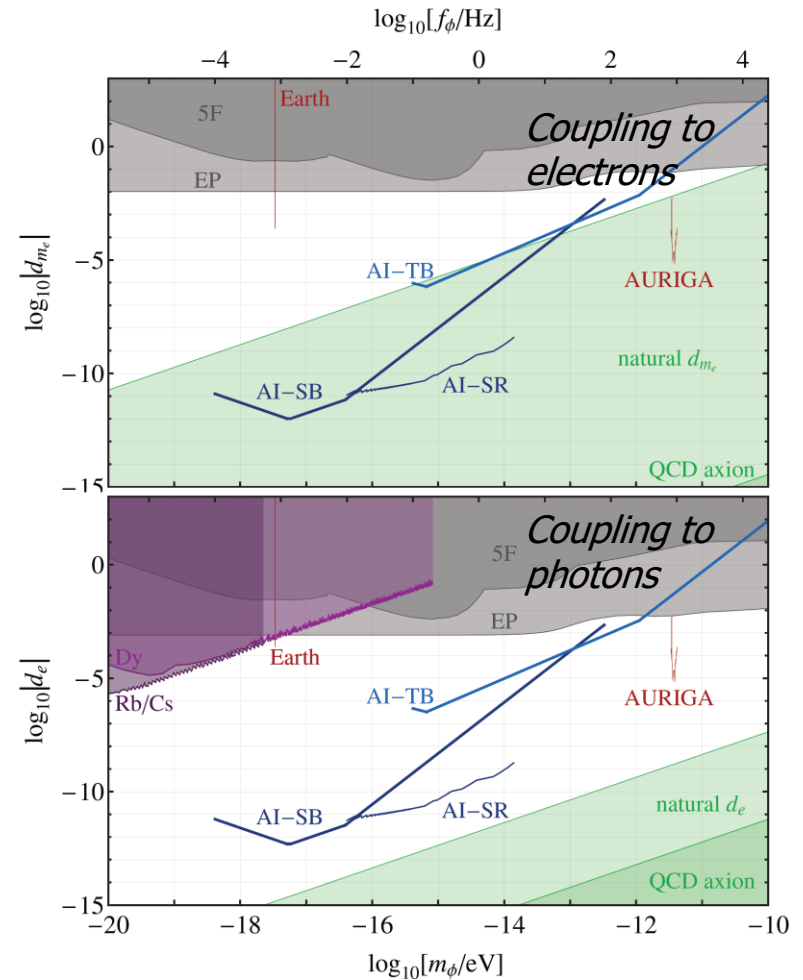


MAGIS-100 GW and DM sensitivity

Gravitational wave (GW) sensitivity

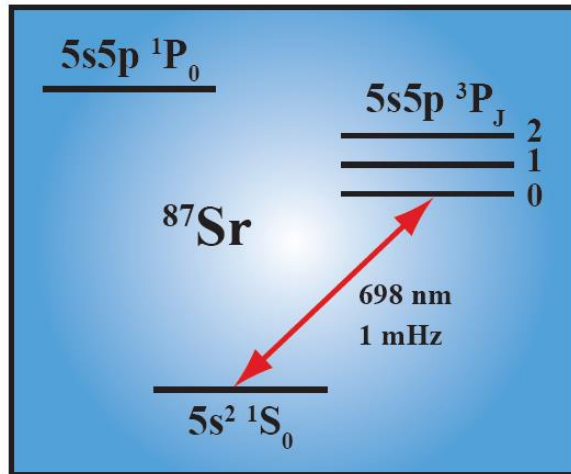


Dark matter (DM) sensitivity



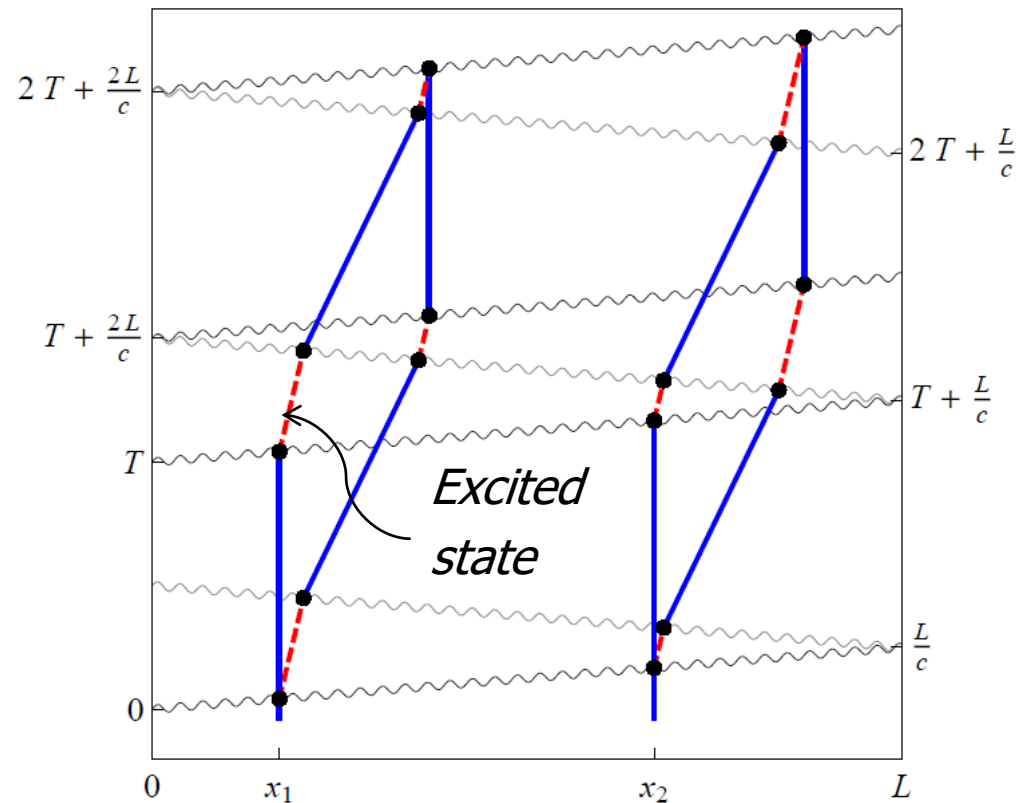
Laser frequency noise insensitive detector

Atomic excitation scheme



Laser phase noise
common to both
interferometers

Atom interferometer and laser
space-time trajectories.

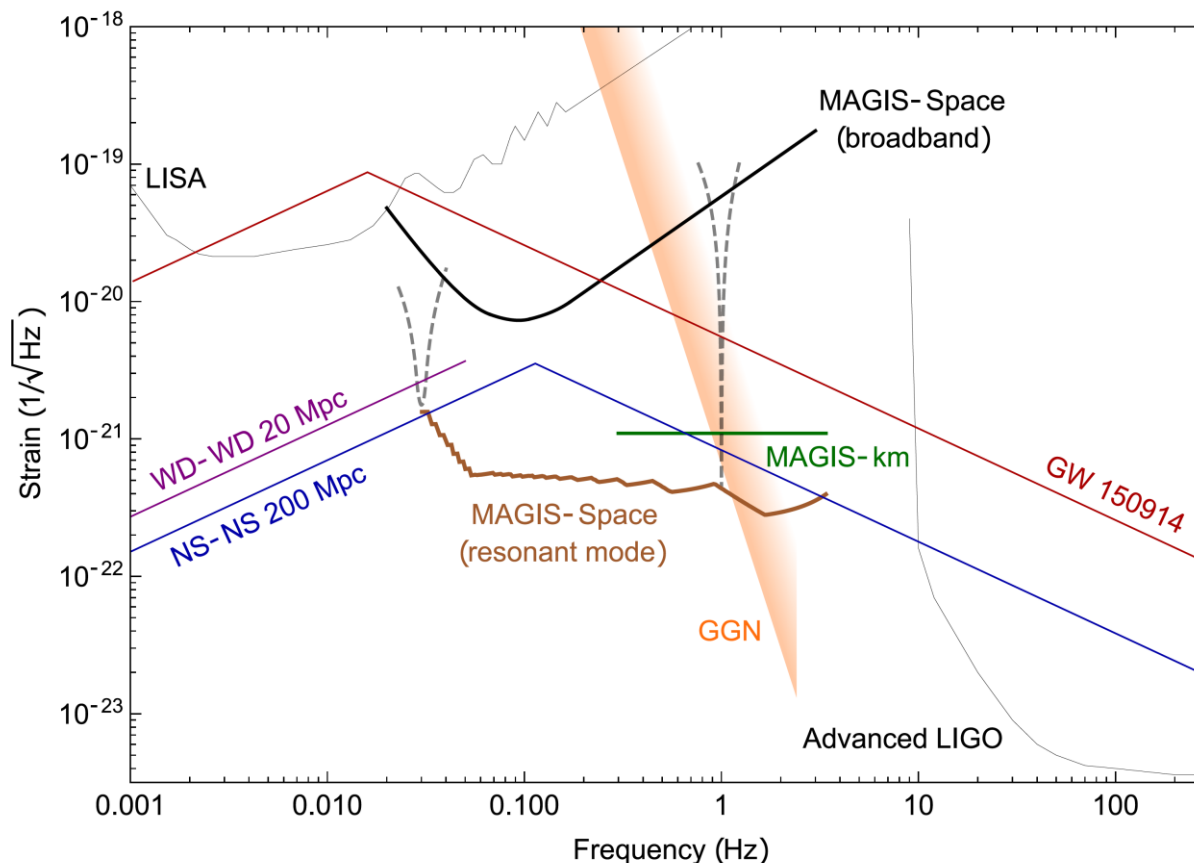


Gravitational wave (GW) response

$$\Delta\phi = \frac{4N\omega_a h}{c} (x_1 - x_2) \sin^2\left(\frac{\omega T}{2}\right) \sin(\phi_0 + \omega T)$$

Atomic transition freq.
GW phase

GW phase shift
for interferometer
pair



Literature: B. Lamine, et al., Eur. Phys. J. D **20**, (2002); R. Chiao, et al., J. Mod. Opt. **51**, (2004); S. Foffa, et al., Phys. Rev. D **73**, (2006); A. Roura, et al., Phys. Rev. D **73**, (2006); P. Delva, Phys. Lett. A **357** (2006); G. Tino, et al., Class. Quant. Grav. **24** (2007), Dimopoulos, et al., PRD (2008), Graham, et al., PRL (2013).



Ultra-light scalar field dark matter detection

PRL 117, 261301 (2016)

PHYSICAL REVIEW LETTERS

week ending
23 DECEMBER 2016

Sensitivity of Atom Interferometry to Ultralight Scalar Field Dark Matter

Andrew A. Geraci and Andrei Derevianko

Department of Physics, University of Nevada, Reno, Nevada 89557, USA

(Received 24 September 2016; published 20 December 2016)

We discuss the use of atom interferometry as a tool to search for dark matter (DM) composed of virialized ultralight fields (VULFs). Previous work on VULF DM detection using accelerometers has considered the possibility of equivalence-principle-violating effects whereby gradients in the dark matter field can directly produce relative accelerations between media of differing composition. In atom interferometers, we find that time-varying phase signals induced by coherent oscillations of DM fields can also arise due to changes in the atom rest mass that can occur between light pulses throughout the interferometer sequence as well as changes in Earth's gravitational field. We estimate that several orders of magnitude of unexplored phase space for VULF DM couplings can be probed due to these new effects.

DOI: 10.1103/PhysRevLett.117.261301

Physical origin of the sensitivity:

$$g(t) = g_0[1 + \delta_g \cos(\omega t + \theta_0)],$$

$$m(t) = m_0[1 + \delta_m \cos(\omega t + \theta_0)],$$

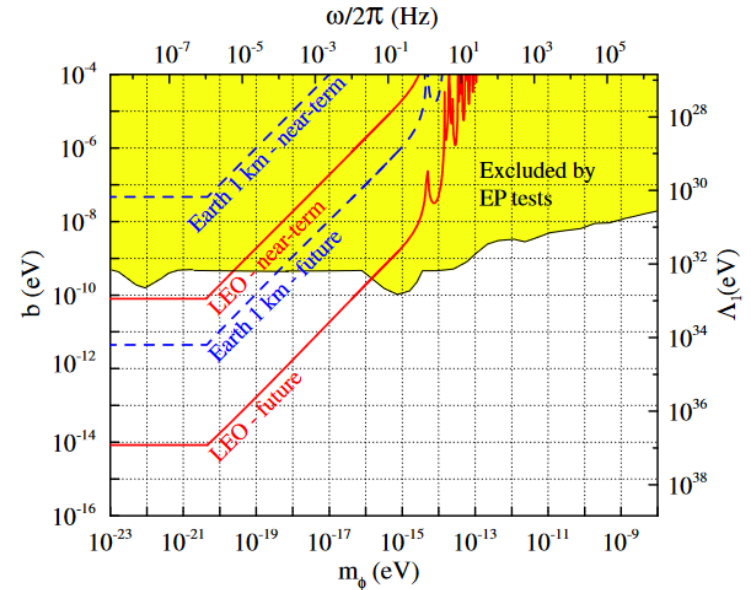
Corresponding atom interferometer response:

$$\Delta\phi \approx -k_{\text{eff}}g_0(1 + \delta_g)T^2 - \delta_m \frac{k_{\text{eff}}}{\omega}(v_L + v_R/2)(\omega T)^3.$$

Also, clock coupling: $\omega_A(t) \simeq \omega_A + \Delta\omega_A \cos(m_\phi t);$

(Arvanitaki et al. 2018)

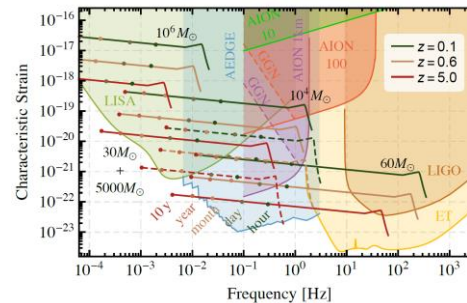
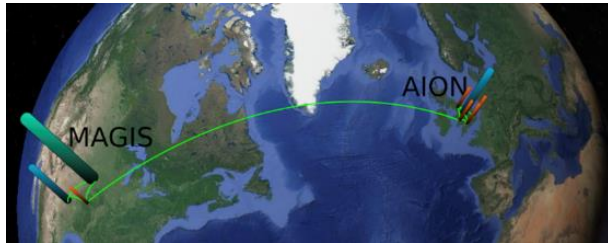
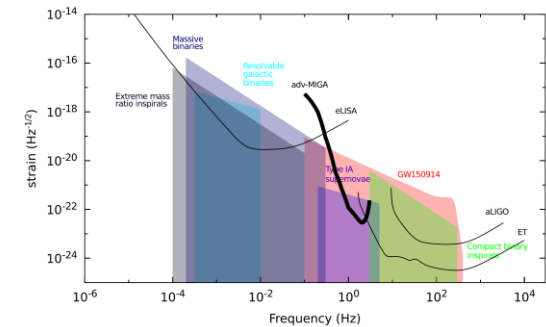
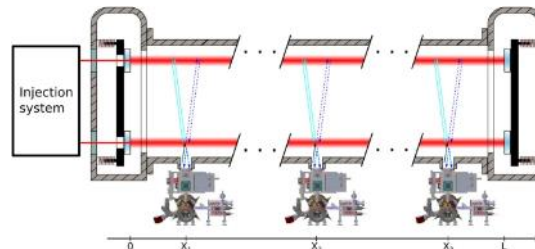
$$\Delta\omega_A \equiv \omega_A \sqrt{4\pi G_N \phi_0} (d_{m_e} + \xi d_e).$$



STANFORD UNIVERSITY

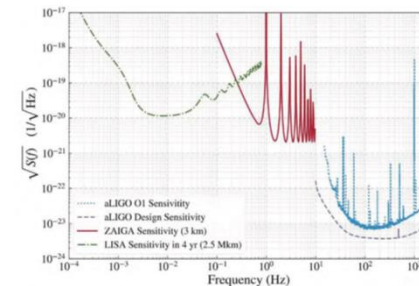
Project	Baseline Length	Number of Baselines	Orientation	Atom	Atom Optics	Location
MAGIS [70]	100 m	1	Vertical	Sr	Clock AI, Bragg	USA
AION [71]	100 m	1	Vertical	Sr	Clock AI	UK
MIGA [5]	200 m	2	Horizontal	Rb	Bragg	France
ZAIGA [8]	300 m	3	Vertical	Rb, Sr	Raman, Bragg, OLC	China

MIGA: Matter Wave laser
Interferometric Gravitation
Antenna (France)



AION: Atom
Interferometer Observatory
and Network (UK)

ZAIGA: Zhaoshan Long-baseline Atom Interferometer Gravitation Antenna (China)



Thanks

Peter Asenbaum
Chris Overstreet
Joe Curti
Minjeong Kim

Peter Graham (Stanford)
Jason Hogan (Stanford)
Tim Kovachy (Northwestern)
Surjeet Rajendran (Johns Hopkins)

